

## $Q^2$ Evolution of the Generalized Gerasimov-Drell-Hearn Integral for the Neutron using a $^3\text{He}$ Target

M. Amarian,<sup>5</sup> L. Auerbach,<sup>20</sup> T. Averett,<sup>6,23</sup> J. Berthot,<sup>4</sup> P. Bertin,<sup>4</sup> W. Bertozzi,<sup>11</sup> T. Black,<sup>11</sup> E. Brash,<sup>16</sup> D. Brown,<sup>10</sup> E. Burtin,<sup>18</sup> J. R. Calarco,<sup>13</sup> G. D. Cates,<sup>15,22</sup> Z. Chai,<sup>11</sup> J.-P. Chen,<sup>6</sup> Seonho Choi,<sup>20</sup> E. Chudakov,<sup>6</sup> E. Cisbani,<sup>5</sup> C. W. de Jager,<sup>6</sup> A. Deur,<sup>4,6,22</sup> R. DiSalvo,<sup>4</sup> S. Dieterich,<sup>17</sup> P. Djawotho,<sup>23</sup> M. Finn,<sup>23</sup> K. Fissum,<sup>11</sup> H. Fonvieille,<sup>4</sup> S. Frullani,<sup>5</sup> H. Gao,<sup>11</sup> J. Gao,<sup>1</sup> F. Garibaldi,<sup>5</sup> A. Gasparian,<sup>3</sup> S. Gilad,<sup>11</sup> R. Gilman,<sup>6,17</sup> A. Glamazdin,<sup>9</sup> C. Glashauser,<sup>17</sup> E. Goldberg,<sup>1</sup> J. Gomez,<sup>6</sup> V. Gorbenko,<sup>9</sup> J.-O. Hansen,<sup>6</sup> F. W. Hersman,<sup>13</sup> R. Holmes,<sup>19</sup> G. M. Huber,<sup>16</sup> E. W. Hughes,<sup>1</sup> T. B. Humensky,<sup>15</sup> S. Incerti,<sup>20</sup> M. Iodice,<sup>5</sup> S. Jensen,<sup>1</sup> X. Jiang,<sup>17</sup> C. Jones,<sup>1</sup> G. M. Jones,<sup>8</sup> M. Jones,<sup>23</sup> C. Jutier,<sup>4,14</sup> A. Ketikyan,<sup>24</sup> I. Kominis,<sup>15</sup> W. Korsch,<sup>8</sup> K. Kramer,<sup>23</sup> K. S. Kumar,<sup>12,15</sup> G. Kumbartzki,<sup>17</sup> M. Kuss,<sup>6</sup> E. Lakurigi,<sup>20</sup> G. Laveissiere,<sup>4</sup> J. Leroise,<sup>6</sup> M. Liang,<sup>6</sup> N. Liyanage,<sup>6,11</sup> G. Lolos,<sup>16</sup> S. Malov,<sup>17</sup> J. Marroncle,<sup>18</sup> K. McCormick,<sup>14</sup> R. McKeown,<sup>1</sup> Z.-E. Meziani,<sup>20</sup> R. Michaels,<sup>6</sup> J. Mitchell,<sup>6</sup> Z. Papandreou,<sup>16</sup> T. Pavlin,<sup>1</sup> G. G. Petratos,<sup>7</sup> D. Pripstein,<sup>1</sup> D. Prout,<sup>7</sup> R. Ransome,<sup>17</sup> Y. Roblin,<sup>4</sup> D. Rowntree,<sup>11</sup> M. Rvachev,<sup>11</sup> F. Sabatie,<sup>14</sup> A. Saha,<sup>6</sup> K. Slifer,<sup>20</sup> P. A. Souder,<sup>19</sup> T. Saito,<sup>21</sup> S. Strauch,<sup>17</sup> R. Suleiman,<sup>7</sup> K. Takahashi,<sup>21</sup> S. Tejiro,<sup>21</sup> L. Todor,<sup>14</sup> H. Tsubota,<sup>21</sup> H. Ueno,<sup>21</sup> G. Urciuoli,<sup>5</sup> R. Van der Meer,<sup>6,16</sup> P. Vernin,<sup>18</sup> H. Voskanian,<sup>24</sup> B. Wojtsekhowski,<sup>6</sup> F. Xiong,<sup>11</sup> W. Xu,<sup>11</sup> J.-C. Yang,<sup>2</sup> B. Zhang,<sup>11</sup> and P. Zolnierczuk<sup>8</sup>

(Jefferson Lab E94010 Collaboration)

<sup>1</sup>California Institute of Technology, Pasadena, California 91125

<sup>2</sup>Chungnam National University, Taejeon 305-764, Korea

<sup>3</sup>Hampton University, Hampton, Virginia 23668

<sup>4</sup>LPC IN2P3/CNRS, Université Blaise Pascal, F-63170 Aubière CEDEX, France

<sup>5</sup>Istituto Nazionale di Fisica Nucleare, Sezione Sanità, 00161 Roma, Italy

<sup>6</sup>Thomas Jefferson National Accelerator Facility, Newport News, Virginia 23606

<sup>7</sup>Kent State University, Kent, Ohio 44242

<sup>8</sup>University of Kentucky, Lexington, Kentucky 40506

<sup>9</sup>Kharkov Institute of Physics and Technology, Kharkov 310108, Ukraine

<sup>10</sup>University of Maryland, College Park, Maryland 20742

<sup>11</sup>Massachusetts Institute of Technology, Cambridge, Massachusetts 02139

<sup>12</sup>University of Massachusetts–Amherst, Amherst, Massachusetts 01003

<sup>13</sup>University of New Hampshire, Durham, New Hampshire 03824

<sup>14</sup>Old Dominion University, Norfolk, Virginia 23529

<sup>15</sup>Princeton University, Princeton, New Jersey 08544

<sup>16</sup>University of Regina, Regina, Canada S4S 0A2

<sup>17</sup>Rutgers, The State University of New Jersey, Piscataway, New Jersey 08855

<sup>18</sup>CEA Saclay, DAPNIA/SPhN, F-91191 Gif sur Yvette, France

<sup>19</sup>Syracuse University, Syracuse, New York 13244

<sup>20</sup>Temple University, Philadelphia, Pennsylvania 19122

<sup>21</sup>Tohoku University, Sendai 980, Japan

<sup>22</sup>University of Virginia, Charlottesville, Virginia 22904

<sup>23</sup>The College of William and Mary, Williamsburg, Virginia 23187

<sup>24</sup>Yerevan Physics Institute, Yerevan 375036, Armenia

(Received 15 May 2002; published 26 November 2002)

We present data on the inclusive scattering of polarized electrons from a polarized  $^3\text{He}$  target at energies from 0.862 to 5.06 GeV, obtained at a scattering angle of  $15.5^\circ$ . Our data include measurements from the quasielastic peak, through the nucleon resonance region, and beyond, and were used to determine the virtual photon cross-section difference  $\sigma_{1/2} - \sigma_{3/2}$ . We extract the extended Gerasimov-Drell-Hearn integral for the neutron in the range of four-momentum transfer squared  $Q^2$  of 0.1–0.9 GeV<sup>2</sup>.

DOI: 10.1103/PhysRevLett.89.242301

PACS numbers: 25.30.-c, 11.55.Hx

Sum rules involving the spin structure of the nucleon offer an important opportunity to study quantum chromodynamics (QCD). At long distance scales or in the confinement regime, a sum rule of great interest is that

due to Gerasimov, Drell, and Hearn (GDH) [1,2]. The GDH sum rule relates an integral over the full excitation spectrum of the spin-dependent total photoabsorption cross section to the nucleon's anomalous magnetic

moment. It has not been investigated experimentally until recently [3], and further measurements are needed for a definitive test. At short distance scales or in the perturbative regime, two other sum rules, one due to Bjorken [4] and the other derived by Ellis and Jaffe [5], have provided significant information on nucleon spin structure through an extensive experimental and theoretical investigation [6]. These sum rules make predictions involving the first moments of the spin structure functions measured in deep inelastic scattering (DIS).

The GDH sum rule pertains strictly to the real photon case for which the four-momentum transfer squared  $Q^2 = 0$ . DIS data, in contrast, are taken at relatively high values of  $Q^2$ . It is desirable to have both experimental and theoretical bridges between these two very different regimes. This was achieved by generalizing the ‘‘GDH integral’’ to include the scattering of virtual photons for which  $Q^2 > 0$  [7]. The GDH integral can be written as

$$\begin{aligned} I(Q^2) &= \int_{\nu_0}^{\infty} \frac{d\nu}{\nu} (1-x) [\sigma_{1/2}(\nu, Q^2) - \sigma_{3/2}(\nu, Q^2)] \\ &= 2 \int_{\nu_0}^{\infty} \frac{d\nu}{\nu} (1-x) \sigma'_{TT}, \end{aligned} \quad (1)$$

where we have chosen this form in order to compare with chiral perturbation theory ( $\chi$ PT) calculations, and alternative generalizations are discussed in [8,9]. Here,  $\sigma_{1/2(3/2)}(\nu, Q^2)$  is the total *virtual* photoabsorption cross section for the nucleon with a projection of  $\frac{1}{2}(\frac{3}{2})$  for the total spin along the direction of photon momentum,  $\nu$  is the electron’s energy loss,  $\nu_0$  is the pion production threshold,  $x = Q^2/2M\nu$  is the Bjorken scaling variable,  $M$  is the mass of the nucleon, and  $\sigma'_{TT}$  is the transverse-transverse interference cross section. As  $Q^2 \rightarrow 0$ ,  $I(Q^2)$  is predicted by the original GDH sum rule:

$$I(0) = -\frac{2\pi^2\alpha}{M^2} \kappa^2, \quad (2)$$

where  $\alpha$  is the fine structure constant and  $\kappa$  is the nucleon’s anomalous magnetic moment. Experimentally, recent measurements have been made on  $I(0)$  for the proton [3], but the neutron has yet to be measured. As  $Q^2 \rightarrow \infty$ ,  $I(Q^2) \rightarrow 16\pi^2\alpha\Gamma_1/Q^2$ , where  $\Gamma_1 = \int_0^1 g_1 dx$  is the first moment of the nucleon’s spin structure function  $g_1$ . Both  $\Gamma_1^p$  for the proton and  $\Gamma_1^n$  for the neutron have been well studied experimentally at high  $Q^2$  [6], and their difference  $\Gamma_1^p - \Gamma_1^n$  is predicted by the Bjorken sum rule. The two limits of the  $Q^2$  evolution of  $I(Q^2)$  are thus constrained by a combination of theory and experimental data.

It has recently been emphasized [8] that the extended GDH integral can be related [8,10,11] to the forward virtual Compton scattering amplitudes, thus establishing a true  $Q^2$  dependent sum rule. The original GDH sum rule and the Bjorken sum rule can both be viewed as special

cases of this ‘‘extended GDH sum rule.’’ The extended GDH sum rule can be tested at any value of  $Q^2$  for which the Compton amplitudes can be computed. Near  $Q^2 = 0$ , where the amplitudes are best understood in terms of hadronic degrees of freedom, several calculations have been performed using  $\chi$ PT [8,11–14]. The two most recent of these efforts, which take different approaches, include next-to-leading order corrections [12–14]. An important issue is the highest values of  $Q^2$  at which the calculations are valid, with estimates ranging as high as  $0.3 \text{ GeV}^2$  [13]. For large  $Q^2$ , a region best described by partonic degrees of freedom, operator product expansion (OPE) techniques have been used to express the Compton amplitudes as a perturbative series in  $\alpha_s$  and a (higher twist) power series in  $1/Q^2$ . The predictions of the Bjorken sum rule can thus be extended to finite  $Q^2$ , perhaps as low as  $Q^2 \sim 0.5 \text{ GeV}^2$  [12]. For lower values of  $Q^2$ , that are still well above the range where  $\chi$ PT is applicable, there is currently little theoretical guidance. This transition region, however, is well suited to the use of lattice QCD [15]. Mapping out  $I(Q^2)$  experimentally, as we have done in this paper for the range of  $0.1 \text{ GeV}^2 \leq Q^2 \leq 0.9 \text{ GeV}^2$ , is an important step to testing these ideas and building our understanding of the dynamics of non-perturbative QCD.

We measured the inclusive scattering of longitudinally polarized electrons from a polarized  $^3\text{He}$  target in Hall A of the Thomas Jefferson National Accelerator Facility (JLab). Data were collected at six incident beam energies: 5.06, 4.24, 3.38, 2.58, 1.72, and 0.86 GeV, all at a nominal scattering angle of  $15.5^\circ$ . The measurements covered values of the invariant mass squared  $W^2 = M^2 + 2M\nu - Q^2$  from the quasielastic peak (not discussed in this paper), through the resonance region, to the values indicated in Fig. 1. Data were taken for both longitudinal and transverse target polarization orientations. Both spin asymmetries and absolute cross sections were measured.

A cw beam of polarized electrons was produced by illuminating a strained GaAs photocathode with circularly polarized light. Beam currents were limited to 10–15  $\mu\text{A}$  to minimize depolarization of the target. The average polarization of the electron beam was  $0.70 \pm 0.03$ , and was monitored using a double arm Møller polarimeter. The polarization was typically reversed at a rate of 1 Hz.

The  $^3\text{He}$  target was polarized by spin exchange with optically pumped rubidium (Rb) [16]. Built specifically for this and subsequent experiments in Hall A, the design of the target is similar to that built at SLAC for E142 [17], but with greater flexibility for polarization direction and the handling of high average beam currents [18,19]. The average in-beam polarization was  $0.35 \pm 0.014$ . The  $^3\text{He}$  gas, at a density corresponding to 10–12 atm at  $0^\circ\text{C}$ , was contained in sealed glass cells together with a small quantity ( $\sim 70$  Torr) of nitrogen. The portion of the cell in the electron beam was a cylinder  $\sim 40$  cm in

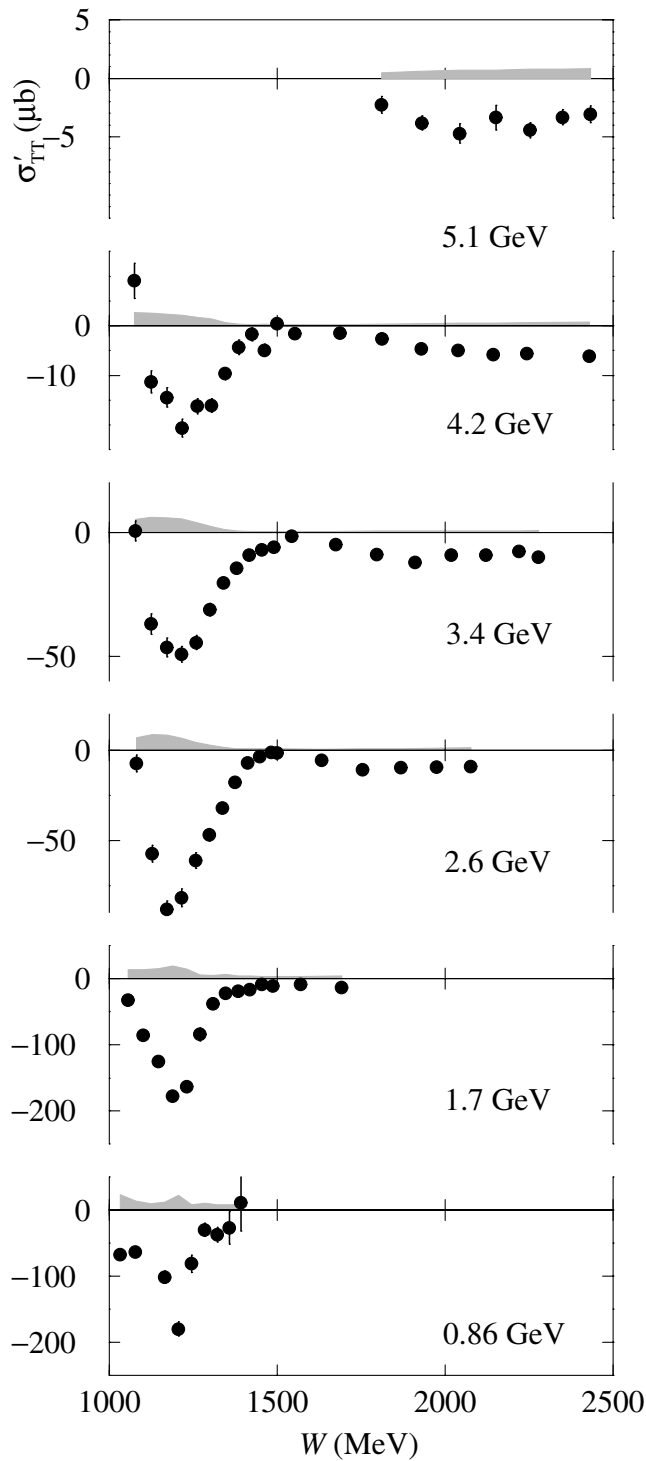


FIG. 1.  $\sigma'_{TT}$  of the neutron in  ${}^3\text{He}$  (see text) is plotted as a function of invariant mass  $W$  for each of the six incident energies studied.

length. Spin exchange took place in a spherical chamber ( $\sim 62$  mm in diameter) that was irradiated with  $\sim 90$  W of light, centered at 795 nm, from high-power diode-laser arrays. The polarization of the  ${}^3\text{He}$  was monitored by the NMR technique of adiabatic fast passage (AFP)

[20]. The NMR system was calibrated by two methods. In one method, the AFP signals of  ${}^3\text{He}$  were compared with the AFP signals from water which had a small polarization due to the usual Boltzmann distribution. In the other method, AFP signals were observed following a determination of the  ${}^3\text{He}$  polarization using a shift of the Rb electron paramagnetic resonance lines due to collisions with polarized  ${}^3\text{He}$  atoms [21]. Independent verification of our target polarimetry at the level of 4% was provided by measuring the asymmetry in elastic scattering [22,23], which depends on the product of the target and beam polarizations.

The scattered electrons were detected using the two Hall A high resolution spectrometers. Momenta were determined by track analysis, and particle identification was accomplished using gas Cerenkov detectors and lead-glass shower counters. Pion rejection was better than  $10^3$  in both spectrometer arms, which was more than sufficient since the  $\pi/e$  ratio was never worse than 10.

The quantities we measure experimentally are related to  $\sigma'_{TT}$  and the transverse-longitudinal interference term  $\sigma'_{LT}$  in the Born approximation according to the relations

$$\frac{d^2\sigma^{\uparrow\uparrow}}{d\Omega dE'} - \frac{d^2\sigma^{\uparrow\downarrow}}{d\Omega dE'} = B(\sigma'_{TT} + \eta\sigma'_{LT}) \quad (3)$$

and

$$\frac{d^2\sigma^{\uparrow\Rightarrow}}{d\Omega dE'} - \frac{d^2\sigma^{\uparrow\Leftarrow}}{d\Omega dE'} = B\sqrt{\frac{2\epsilon}{1+\epsilon}}(\sigma'_{LT} - \zeta\sigma'_{TT}), \quad (4)$$

where  $d^2\sigma^{\uparrow\uparrow(\uparrow\downarrow)}/d\Omega dE'$  is the cross section for the case in which the beam and target spin directions are antiparallel (parallel), and the left side of (4) represents the corresponding quantity for transverse target spin orientation. Also  $B = 2(\alpha/4\pi^2)(K/Q^2)(E'/E)[2/(1-\epsilon)] \times (1-E'\epsilon/E)$ , where  $E$  and  $E'$  are the initial and final electron energies,  $\epsilon^{-1} = 1 + 2[1 + Q^2/4M^2x^2] \times \tan^2(\theta/2)$ ,  $\theta$  is the scattering angle in the laboratory frame,  $\eta = \epsilon\sqrt{Q^2}/(E - E'\epsilon)$ , and  $\zeta = \eta(1 + \epsilon)/2\epsilon$ . The factor  $K$  represents the virtual photon flux and is convention dependent. We use the convention  $K = \nu - Q^2/2M$  [24].

To extract from our raw  ${}^3\text{He}$  data  $\sigma'_{TT}$ , which is defined within the Born approximation, we must first apply “radiative corrections” to account for the emission of real and virtual photons. These corrections were performed using the procedure first described by Mo and Tsai for the case of unpolarized scattering [25], and extended to include polarized effects using the program POLRAD [26]. For our experiment, we incorporated into POLRAD our actual data for the quasielastic and resonance regions, as their effect on the radiative corrections are significant. The results for  $\sigma'_{TT}$  are shown in Fig. 1 as a function of the invariant mass  $W$  for each of the six energies measured, and represent the neutron to the extent that we have set  $M$  equal to the neutron mass in Eqs. (3)

and (4). We note, though, that for  $\sigma'_{TT}$ , no corrections for nuclear effects were applied, so the quantity plotted is different from the corresponding quantity for the free neutron.

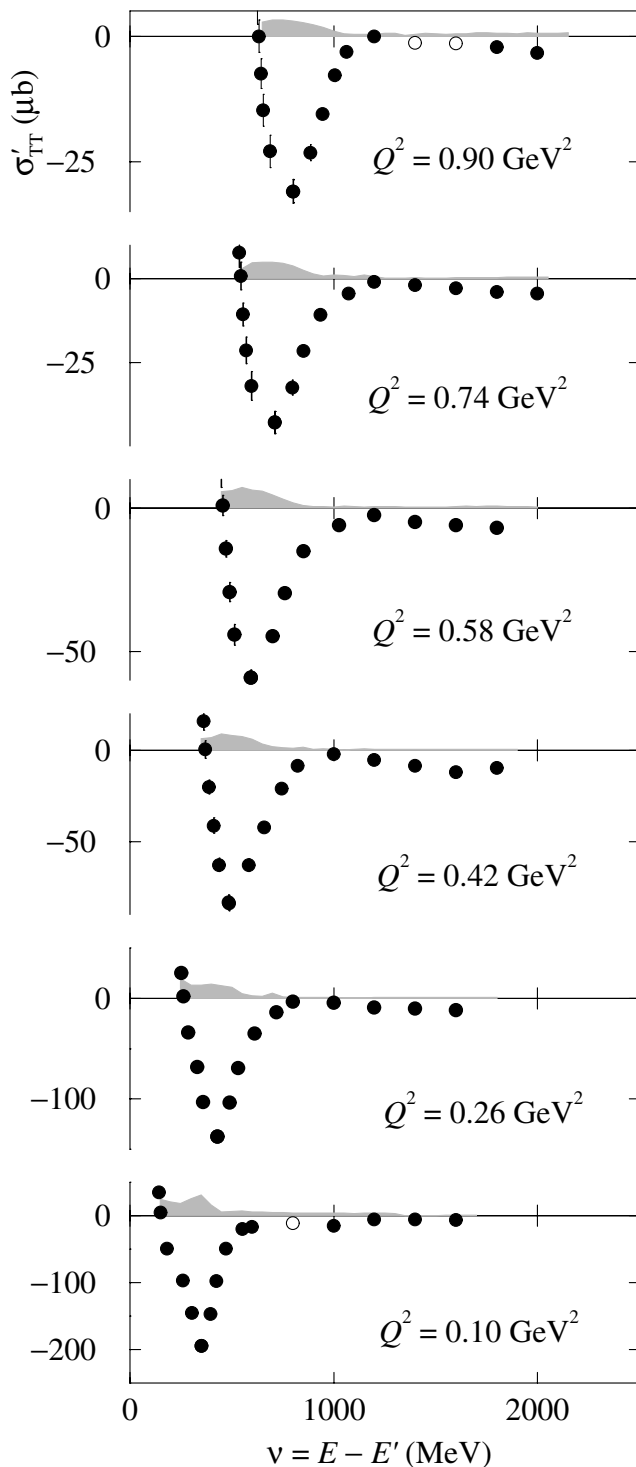


FIG. 2.  $\sigma'_{TT}$  of the neutron in  ${}^3\text{He}$  (see text) is plotted as a function of energy loss  $\nu$  for each of six values of constant  $Q^2$ . The points shown with solid (open) circles were determined by interpolation (extrapolation).

The error bars are due to statistics only, with the grey bands indicating systematic errors. The error due to radiative corrections is on average about half of the systematic error on  $\sigma'_{TT}$ , and was determined by considering a wide variety of initial starting points for POLRAD. The variation in the radiative corrections was always less than 20%, which we took to be the uncertainty in the correction. At 0.86 GeV, we had no data at lower energies and were forced to use several models as starting points for POLRAD. We found variations of less than 40% in the correction, which we took to be the uncertainty. Other systematic errors included a relative uncertainty of 5% from absolute cross section, 4% from target polarization, and 4% from beam polarization.

To compute  $I(Q^2)$ ,  $\sigma'_{TT}$  is needed at constant  $Q^2$ . We chose six equally spaced values of  $Q^2$  in the range  $0.1 \text{ GeV}^2 \leq Q^2 \leq 0.9 \text{ GeV}^2$  and determined  $\sigma'_{TT}$  from our measured points by interpolation or, for a few points, extrapolation. The results are plotted in Fig. 2 as a function of  $\nu$ . The prominent peak in the cross section is the  $\Delta_{1232}$  resonance. The error bars represent the uncertainty due to statistics, and the grey bands indicate the uncertainty due to systematic errors which, in addition to those shown in Fig. 1, include contributions from interpolation and extrapolation.

The extended GDH integral was computed for each value of  $Q^2$  according to Eq. (1) using limits of integration extending from the nominal nucleon pion threshold to a value of  $\nu$  corresponding to  $W = 2.0 \text{ GeV}$ . The contribution due to the quasielastic tail, and the effect of varying the lower limit of integration (to account for below-threshold pion production) were both studied and the full variation observed was included as part of our systematic error. The results are given in Table I. In plotting our results, we have applied a correction to account for the fact that our neutron was embedded in a  ${}^3\text{He}$  nucleus. We have used a calculation due to Ciofi degli Atti and Scopetta [27], the only calculation available in the resonance region. The estimated uncertainty of the correction within their model ranged from around 10% at  $Q^2 = 0.1 \text{ GeV}^2$  to around 5% or less for  $Q^2 \geq 0.5 \text{ GeV}^2$ . Our results for  $I(Q^2)$  for the neutron, with the integration covering roughly the resonance region, are shown in Fig. 3 using open circles. The error bars, when visible, represent

TABLE I. Measured values for  $I(Q^2)$  prior to nuclear corrections together with statistical and systematic errors.

$Q^2$ (GeV $^2$ )	$I_{\text{GDH}}$ ( $\mu\text{b}$ )	Statistical ( $\mu\text{b}$ )	Systematic ( $\mu\text{b}$ )
0.10	-187.50	5.23	28.43
0.26	-109.92	2.04	13.77
0.42	-53.51	1.21	5.48
0.58	-31.68	0.74	3.72
0.74	-18.27	0.64	2.42
0.90	-10.47	0.46	1.52

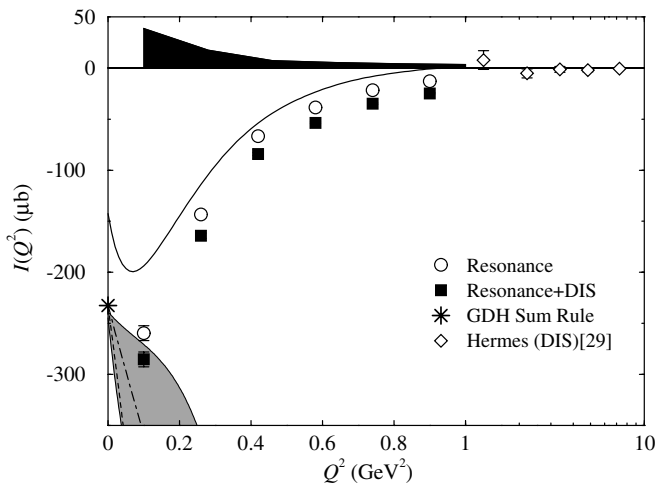


FIG. 3. Our measurements for  $I(Q^2)$  vs  $Q^2$ , both with and without an estimate of the DIS contribution. Also shown with a dotted (dot-dashed) line are the  $\chi$ PT calculations of Ref. [12] (Refs. [13,14]). The calculation of Ref. [9], based largely on the MAID model, is shown with a solid line. We include data from HERMES [29] and, to avoid compressing our horizontal scale, we use a semilog scale for  $Q^2 > 1 \text{ GeV}^2$ .

statistical uncertainties only, and the systematic effects are shown with a black band. We have made an estimate of the unmeasured strength in  $I(Q^2)$  for the region  $4 \text{ GeV}^2 < W^2 < 1000 \text{ GeV}^2$  using the parametrization of Thomas and Bianchi [28] ( $1000 \text{ GeV}^2$  was the highest value considered in their paper). The solid squares have this estimate included, and an estimate of the theoretical uncertainty has already been included in the systematic error shown.

Our data indicate a smooth variation of  $I(Q^2)$  to increasingly negative values as  $Q^2$  varies from  $0.9 \text{ GeV}^2$  toward zero. Our data are more negative than the prediction of Drechsel, Kamalov, and Tiator, whose calculation is mostly based on the phenomenological model MAID, and is shown on Fig. 3 as a solid line [9]. Their prediction includes contributions to  $I(Q^2)$  for  $W \leq 2 \text{ GeV}$ , and should thus be compared with the open circles. At high  $Q^2$ , our data approach those of HERMES, which spans the range  $1.28 \text{ GeV}^2 < Q^2 < 7.25 \text{ GeV}^2$  [29], but includes only the DIS part of the GDH integral. It is desirable to compare our data with the GDH sum rule prediction  $I(0) = -232.8 \mu\text{b}$ . This prediction is indicated in Fig. 3, along with extensions to  $Q^2 > 0$  using two  $\chi$ PT calculations, that described in [12] (dotted line) and collectively in [13,14] (dot-dashed line). Also shown with the grey band is a range of values of  $I(Q^2)$  that would result from a  $\chi$ PT theory calculation including certain resonance effects, where the range shown is due to the uncertainty in certain resonance parameters [14]. We find the overlap of our lowest  $Q^2$  point with the grey band encouraging, and look forward to both further calculations as well as further measurements [30].

In conclusion, we have made the first measurements of  $\sigma'_{TT}$  and the generalized GDH integral  $I(Q^2)$  of the neutron at low  $Q^2$  ( $0.1 \text{ GeV}^2 \leq Q^2 \leq 0.9 \text{ GeV}^2$ ). The data show a dramatic change in the value of the integral from what is observed at high  $Q^2$  ( $0.9 \text{ GeV}^2 < Q^2$ ). While not unexpected from phenomenological models, our data illustrate the sensitivity of  $I(Q^2)$  to the transition from partonic to hadronic behavior. Our data provide a precision data base for twist expansion analysis, a check of  $\chi$ PT calculations, and establish an important benchmark against which one can compare future calculations and measurements of low  $Q^2$  spin structure.

We acknowledge the untiring support of the JLab staff. This work was supported by the U.S. Department of Energy (DOE), the DOE-EPSCoR, the U.S. National Science Foundation, NSERC of Canada, the European INTAS Foundation, the Italian INFN, and the French CEA, CNRS, and Conseil Régional d'Auvergne. The Southeastern Universities Research Association (SURA) operates the Thomas Jefferson National Accelerator Facility for the DOE under Contract No. DE-AC05-84ER40150.

- [1] S. B. Gerasimov, *Sov. J. Nucl. Phys.* **2**, 430 (1966).
- [2] S. D. Drell and A. C. Hearn, *Phys. Rev. Lett.* **16**, 908 (1966).
- [3] GDH and A2 Collaborations, J. Ahrens *et al.*, *Phys. Rev. Lett.* **87**, 022003 (2001).
- [4] J. D. Bjorken, *Phys. Rev.* **148**, 1467 (1966); *Phys. Rev. D* **1**, 1376 (1970).
- [5] J. Ellis and R. L. Jaffe, *Phys. Rev. D* **9**, 1444 (1974); *Phys. Rev. D* **10**, 1669E (1974).
- [6] See, for instance, E. W. Hughes and R. Voss, *Annu. Rev. Nucl. Part. Sci.* **49**, 303 (1999); B. W. Filippone and X. Ji, *Adv. Nucl. Phys.* **26**, 1 (2001), and references therein.
- [7] M. Anselmino, B. L. Ioffe, and E. Leader, *Sov. J. Nucl. Phys.* **49**, 136 (1989).
- [8] X. Ji and J. Osborne, *J. Phys. G* **27**, 127 (2001).
- [9] D. Drechsel, S. S. Kamalov, and L. Tiator, *Phys. Rev. D* **63**, 114010 (2001). Note, model  $I_A$  is plotted in Fig. 3.
- [10] B. L. Ioffe, *Hard Processes* (North-Holland, Amsterdam, 1984), Vol. 1.
- [11] V. Bernard, N. Kaiser, and Ulf-G. Meißner, *Phys. Rev. D* **48**, 3062 (1993); *Int. J. Mod. Phys. E* **4**, 193 (1995).
- [12] X. Ji, C. Kao, and J. Osborne, *Phys. Lett. B* **472**, 1 (2000).
- [13] V. Bernard, T. R. Hemmert, and Ulf-G. Meißner, *Phys. Lett. B* **545**, 105 (2002).
- [14] V. Bernard and Ulf-G. Meißner (private communication).
- [15] Nathan Isgur *et al.*, a proposal submitted to the U.S. Department of Energy (unpublished).
- [16] See, for instance, T. G. Walker and W. Happer, *Rev. Mod. Phys.* **69**, 629 (1997), and references therein.
- [17] SLAC E-142 Collaboration, P. L. Anthony *et al.*, *Phys. Rev. Lett.* **71**, 959 (1993); *Phys. Rev. D* **54**, 6620 (1996).
- [18] J. S. Jensen, Ph.D. thesis, California Institute of Technology, 2000; I. Kominis, Ph.D. thesis, Princeton University, 2000.

- 
- [19] Details of JLab E94-010 and relevant theses can be found at [www.jlab.org/e94010/](http://www.jlab.org/e94010/).
- [20] A. Abragam, *Principles of Magnetic Resonance* (Oxford University Press, Oxford, 1961).
- [21] M.V. Romalis and G.D. Cates, *Phys. Rev. A* **58**, 3004 (1998).
- [22] A. Deur, Ph.D. thesis, Université Blaise Pascal, 2000.
- [23] JLab E95-001 Collaboration, W. Xu *et al.*, *Phys. Rev. Lett.* **85**, 2900 (2000).
- [24] L. N. Hand, *Phys. Rev.* **129**, 1834 (1963).
- [25] L.W. Mo and Y.S. Tsai, *Rev. Mod. Phys.* **41**, 205 (1969); Y.S. Tsai, Report No. SLAC-PUB-848, 1971.
- [26] I.V. Akushevich and N. M. Shumeiko, *J. Phys. G* **20**, 513 (1994).
- [27] C. Ciofi degli Atti and S. Scopetta, *Phys. Lett. B* **404**, 223 (1997).
- [28] N. Bianchi and E. Thomas, *Phys. Lett. B* **450**, 439 (1999); *Nucl. Phys. (Proc. Suppl.)* **B82**, 256 (2000); S.D. Bass and M.M. Brisudova, *Eur. Phys. J. A* **4**, 251 (1999).
- [29] HERMES Collaboration, K. Ackerstaff *et al.*, *Phys. Lett. B* **444**, 531 (1998).
- [30] See, for example, Jefferson Laboratory Proposal E97-110, J.-P. Chen, A. Deur, and F. Garibaldi, spokespersons.